# A review of experimental results at the knee

**Jörg R. Hörandel**

Institute for Experimental Nuclear Physics, University of Karlsruhe, P.O. Box 3640, 76021 Karlsruhe, Germany

E-mail: hoerandel@ik.fzk.de

**Abstract.** Results of experiments investigating air showers in the energy region of the knee are summarized. The all-particle energy spectrum, the mean logarithmic mass, and the average depth of the shower maximum will be discussed. Spectra for groups of elements from air shower data are compared to results from direct measurements.

## 1. Introduction

One of the most remarkable structures in the energy spectrum of cosmic rays is a change of the spectral index $\gamma$ of the power law $dN/dE \propto E^{\gamma}$ at an energy of about 4 PeV, the so called *knee*. In the literature various reasons for the origin of the *knee* are discussed [1]. Some popular concepts are: The maximum energy attained during the acceleration at supernova remnant shock waves [2, 3, 4, 5, 6], reacceleration in the galactic wind [7], acceleration in pulsars [8], or leakage of particles from the Galaxy during the propagation process [9, 10, 11, 12, 13, 14]. Different scenarios are the acceleration of cosmic rays in $\gamma$-ray bursts [15, 16, 17]. During the propagation through the Galaxy cosmic-ray particles are proposed to interact with dense photon fields close to the sources or with background neutrinos [18, 19, 20, 21]. As a last possibility, new processes between elementary particles in the atmosphere are postulated which may transfer energy into non-observed channels and thus cause a *knee* in the observed air shower components [22, 23, 24].

An answer to the question of the cause for the *knee* is expected to reveal also crucial information on the origin of galactic cosmic rays. Experimental access to such questions is provided by measurements of charged cosmic rays (the classical nucleonic component) and $\gamma$-rays with experiments above the atmosphere and by the observation of air showers initiated by high-energy particles in the atmosphere.

A wealth of information on potential cosmic-ray sources is provided by recent measurements of TeV $\gamma$-rays from shell type supernova remnants with the H.E.S.S. experiment [25]. The observations reveal a shell structure of the remnant and an energy spectrum of $\gamma$-rays $\propto E^{-2.2}$ in agreement with the idea of particle acceleration in the shock front. The spectrum extends up to energies of 10 TeV and provides evidence for

the existence of particles with energies beyond 100 TeV at the shock front that emerged from the supernova explosion.

The gyromagnetic radius of a proton with an energy of 1 PeV in the galactic magnetic fields is about 0.4 pc and consequently the probability to detect a source in charged galactic cosmic rays is rather small. Indeed, observations by the KASCADE experiment did not reveal any significant evidence for point sources in the energy range from 0.3 to about 100 PeV [26]. Nevertheless, information on the sources is derived from detailed measurements of the cosmic-ray composition. Investigations of the abundance of refractory nuclides reveal that their abundance at the sources is extremely similar to the abundance observed in the solar system [27]. This indicates that cosmic rays are accelerated from a well-mixed sample of contemporary interstellar matter.

Information on the propagation of particles through the Galaxy is obtained by measurements of the ratio from primary to secondary nuclei, the latter are produced in spallation reactions of cosmic rays with particles of the interstellar medium, and the abundance of radioactive nuclides in cosmic rays. Measurements by the CRIS experiment yield a residence time for cosmic rays in the Galaxy of $15 \cdot 10^6$ yrs and a propagation path length of about 10 g/cm$^2$ for particles with GeV energies [28]. The measured abundances at GeV energies are frequently described using leaky-box models. At higher energies measurements of anisotropy amplitudes yield information on the propagation process [29]. They indicate that the propagation can be described by diffusion models, while leaky-box models exhibit too large anisotropy values even at relatively low energies.

At PeV and EeV energies, information is derived from the measurements of the energy spectrum and mass composition of cosmic rays. In the following, experimental results are reviewed on the all-particle energy spectrum (Sect. 2), the average mass composition (Sect. 3), and spectra for elemental groups (Sect. 4).

## 2. All-particle energy spectrum

The all-particle energy spectra obtained by many experiments are compiled in Fig. 1. Shown are results from direct measurements above the atmosphere as well as from various air shower experiments. The individual measurements agree within a factor of two in the flux values and a similar shape can be recognized for all experiments with a *knee* at energies of about 4 PeV. Typical values for the systematic uncertainties of the absolute energy scale for air shower experiments are about 15 to 20%. Renormalizing the energy scales of the individual experiments to match the all-particle spectrum obtained by direct measurements in the energy region up to almost a PeV requires correction factors in the order of $\pm 10\%$ [60]. A remarkable result, indicating that behind an absorber of 11 hadronic interaction lengths or 30 radiation lengths the energy of the primary particle is determined with an absolute error in the order of $\pm 10\%$. One should keep in mind that the experiments investigate different air shower components, are situated at different atmospheric depths, and use different interactions models to

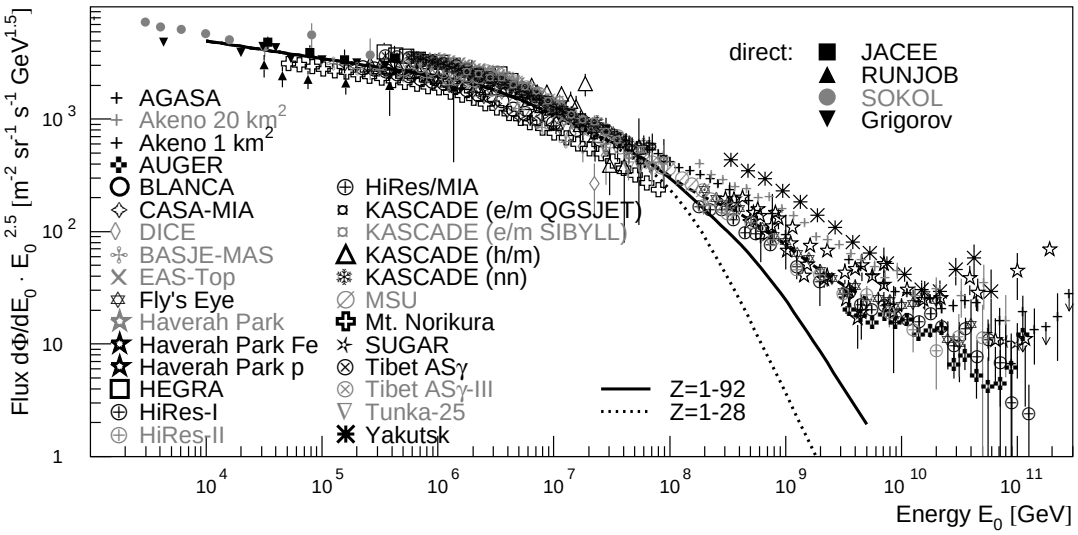


**Figure 1.** All-particle energy spectrum. Results from direct measurements by Grigorov *et al* [30], JACEE [31], RUNJOB [32], and SOKOL [33] as well as from the air shower experiments AGASA [34] Akeno 1 km$^2$ [35] and 20 km$^2$ [36], AUGER [37], BASJE-MAS [38], BLANCA [39], CASA-MIA [40], DICE [41], EAS-TOP [42], Fly's Eye [43], Haverah Park (1991) [44] and (2003) [45], HEGRA [46], HiRes-MIA [47], HiRes-I [48], HiRes-II [49], KASCADE electrons and muons interpreted with two hadronic interaction models [50], hadrons [51], and a neural network analysis combining different shower components [52], MSU [53], Mt. Norikura [54], SUGAR [55], Tibet AS$\gamma$ [56] and AS$\gamma$-III [57], Tunka-25 [58], and Yakutsk [59]. The lines indicate the spectrum according to the *poly-gonato* model.

interpret the observed data. Nevertheless, the systematic differences are relatively small and the all-particle spectrum seems to be well known. Average experimental fluxes are tabulated in [60].

The lines in Fig. 1 indicate sum spectra obtained by extrapolations of the energy spectra for individual elements from direct measurements assuming power laws with a cut-off proportional to the charge of the respective element according to the *poly-gonato* model [60]. Sum spectra for elements from hydrogen to nickel and for all elements are shown. The extrapolated all-particle flux is compatible with the flux derived from air shower experiments in the *knee* region. Above $10^8$ GeV the flux of galactic cosmic rays is not sufficient to account for the observed all particle spectrum, and an additional, presumably extragalactic component is required.

## 3. Average mass of cosmic rays

At energies below a PeV energy spectra for individual elements have been observed above the atmosphere [69]. At higher energies this is presently not possible due to the low flux values and the large fluctuations in the development of extensive air showers. Thus, mostly the mean mass is investigated. An often-used quantity to characterize the composition above 1 PeV is the mean logarithmic mass, defined as $\langle \ln A \rangle = \sum_i r_i \ln A_i$,

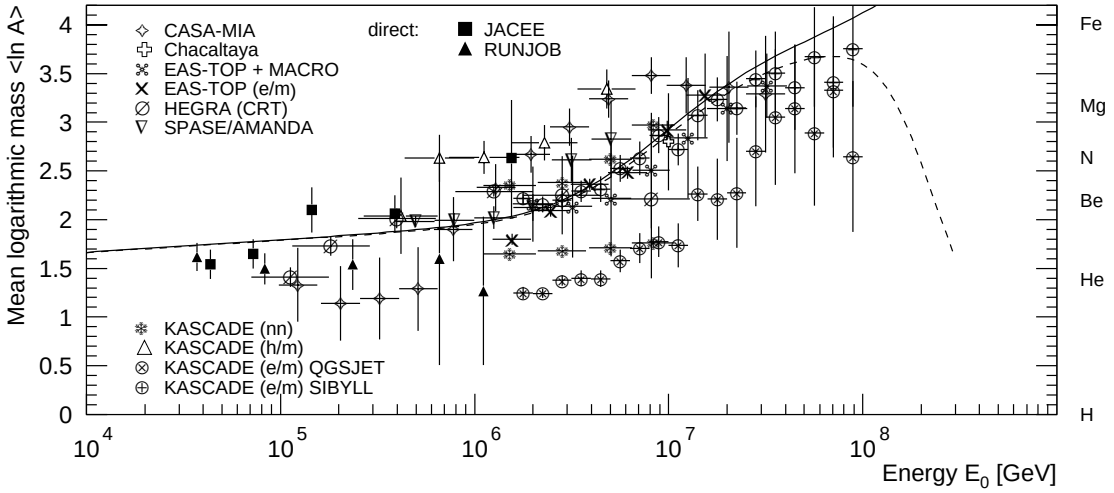


**Figure 2.** Mean logarithmic mass of cosmic rays derived from the measurements of electrons, muons, and hadrons at ground level. Results are shown from CASA-MIA [61], Chacaltaya [62], EAS-TOP electrons and GeV muons [63], EAS-TOP/MACRO (TeV muons) [64], HEGRA CRT [65], KASCADE electrons and muons interpreted with two hadronic interaction models [50], hadrons and muons [66], as well as an analysis combining different observables with a neural network [52], and SPASE/AMANDA [67]. The lines indicate expectations according to the *poly-gonato* model. For comparison, results from direct measurements are shown as well from the JACEE [68] and RUNJOB [32] experiments.

$r_i$ being the relative fraction of nuclei of mass $A_i$. In the superposition model of air showers, the shower development of nuclei with mass $A$ and energy $E_0$ is described by the sum of $A$ proton showers of energy $E = E_0/A$. The shower maximum $t$ penetrates into the atmosphere as $t \propto \ln E$, hence, most air shower observables at ground level scale proportional to $\ln A$.

Frequently, the ratio of the number of electrons and muons is used to determine the mass composition. The experiments CASA-MIA [61], EAS-TOP [63], or KASCADE use muons with an energy of several 100 MeV to 1 GeV. To study systematic effects two hadronic interaction models are used to interpret the data measured with KASCADE [50]. High energy muons detected deep below rock or antarctic ice are utilized by the EAS-TOP/MACRO [64] and SPASE/AMANDA [67] experiments. Also the correlation between the hadronic and muonic shower components has been investigated by KASCADE [66]. The production height of muons has been reconstructed by HEGRA/CRT [65] and KASCADE [70].

Results from various experiments measuring electrons, muons, and hadrons at ground level are compiled in Fig. 2. At low energies the values for the mean logarithmic mass are compared to results from direct measurements. A clear increase as function of energy can be recognized. The experimental values follow a trend predicted by the *poly-gonato* model as indicated by the lines in the figure. However, individual experiments exhibit systematic deviations of about $\pm 1$ unit in $\langle \ln A \rangle$ from the line. Of particular interest are also the investigations of the KASCADE experiment, interpreting the same

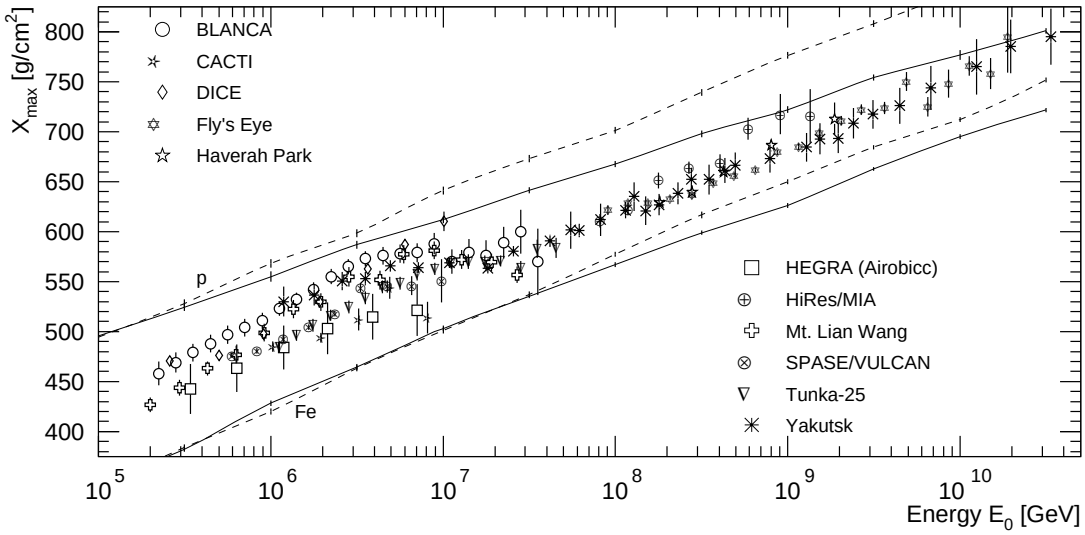


**Figure 3.** Average depth of the shower maximum $X_{max}$ as function of primary energy as obtained by BLANCA [39], CACTI [71], DICE [41], Fly's Eye [43], Haverah Park [72], HEGRA [46], HiRes/MIA [73], Mt. Lian Wang [74], SPASE/VULCAN [75], Tunka-25 [58], and Yakutsk [76]. The lines indicate simulations for proton and iron induced showers using the CORSIKA code with the hadronic interaction model QGSJET 01 (solid line) and a version with lower cross sections and slightly increased elasticities (dashed line, model 3 in [77]).

measured data with two different models for the interactions in the atmosphere results in a systematic difference of about 0.7 to 1 in $\langle \ln A \rangle$.

Another technique to determine the mass of cosmic rays are measurements of the average depth of the shower maximum using non-imaging and imaging Čerenkov detectors as well as fluorescence telescopes at the highest energies. The results of several experiments are presented in Fig. 3 as function of energy. The observed values are compared to predictions of air shower simulations for primary protons and iron nuclei using the program CORSIKA [78] with the hadronic interaction model QGSJET 01 [79] and a modified version with lower cross sections and larger values for the elasticity of the hadronic interactions (model 3a in [77]). The latter is compatible with measurements at colliders, for details see [77]. The lower values for the total inelastic proton-antiproton cross sections yield also lower inelastic proton-air cross sections, which are in good agreement with recent measurements from the HiRes experiment [80, 81]. In principle, the difference between the solid and the dashed lines in the figure represents an estimate of the projection of the experimental errors from collider experiments on the average depth of the shower maximum in air showers. At $10^9$ GeV the difference between the two model versions for primary protons is about half the difference between proton and iron induced showers. This illustrates the significance of the uncertainties of the collider measurements for air shower observables.

Knowing the average depth of the shower maximum for protons $X^p_{max}$ and iron nuclei $X^{Fe}_{max}$ from simulations, the mean logarithmic mass is derived in the superposition

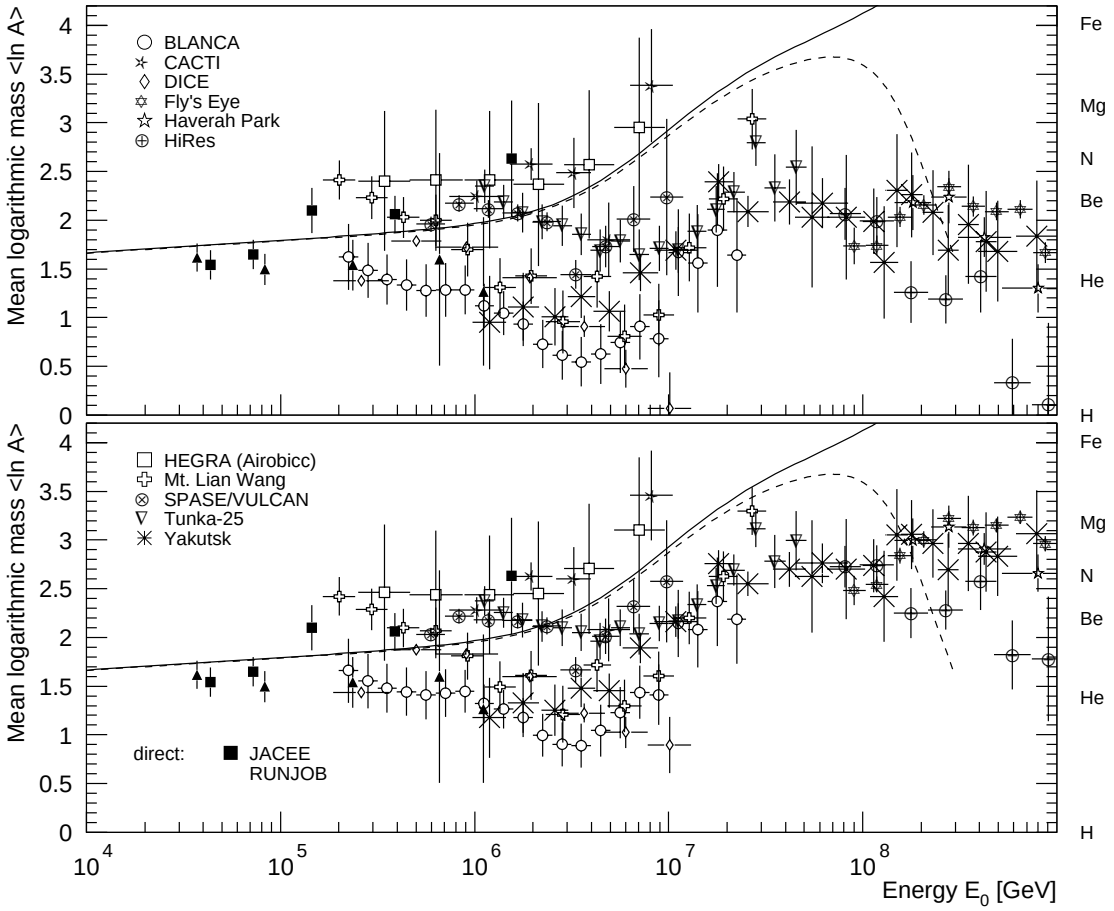


**Figure 4.** Mean logarithmic mass of cosmic rays derived from the average depth of the shower maximum, see Fig. 3. Two hadronic interaction models are used to interpret the measurements: QGSJET 01 (top) and a modified version with lower cross sections and a slightly increased elasticity (model 3a [77], bottom). For references, see caption of Fig. 3. For comparison, results from direct measurements are shown as well from the JACEE [68] and RUNJOB [32] experiments. The lines indicate expectations according to the *poly-gonato* model.

model of air showers from the measured $X_{max}^{meas}$ using $\langle \ln A \rangle = (X_{max}^{meas} - X_{max}^{p})/(X_{max}^{Fe} - X_{max}^{p}) \cdot \ln A_{Fe}$. The corresponding $\langle \ln A \rangle$ values, obtained from the results shown in Fig. 3, are plotted in Fig. 4 versus the primary energy using both interaction models to interpret the observed data. Up to about a PeV there are only marginal differences between the two interpretations. On the other hand, at large energies a significantly heavier composition is obtained for the modified version (model 3a). At $10^9$ GeV the differences amount to about 1 in $\langle \ln A \rangle$. These examples illustrate how strong the interpretation of air shower measurements depends on model parameters such as the inelastic cross sections or elasticities used. At Tevatron energies the cross sections vary within the error range given by the experiments and at $10^8$ GeV the proton air cross sections of QGSJET and model 3a differ only by about 10%, but the general trend of the emerging $\langle \ln A \rangle$ distributions proves to be significantly different. This underlines the importance to test and improve the understanding of hadronic interactions in the

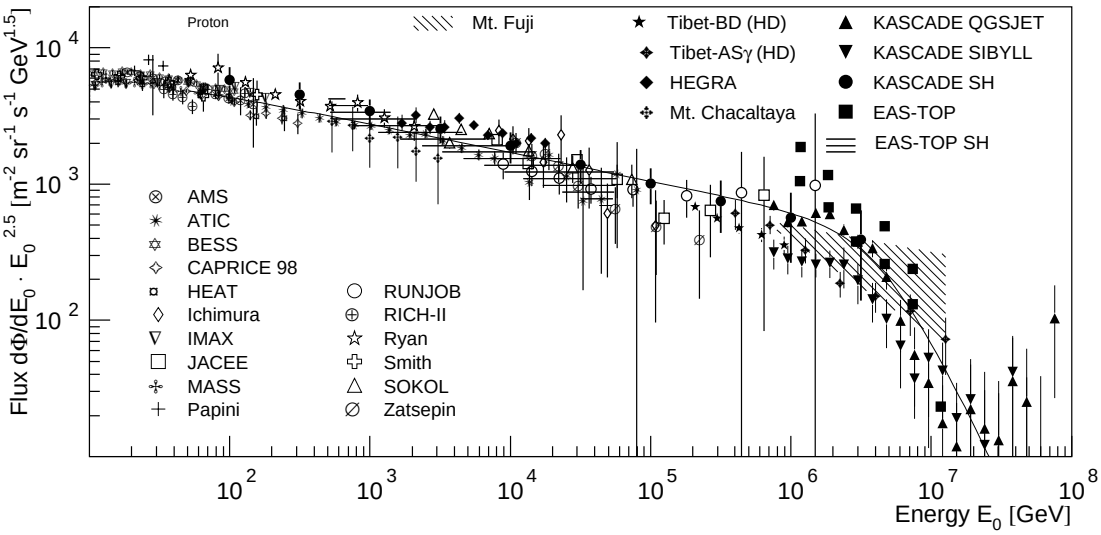


**Figure 5.** Energy spectrum for protons. Results from direct measurements above the atmosphere by AMS [83], ATIC [84], BESS [85], CAPRICE [86], HEAT [87], Ichimura *et al* [88], IMAX [89], JACEE [90], MASS [91], Papini *et al* [92], RUNJOB [32], RICH-II [93], Ryan *et al* [94], Smith *et al* [95], SOKOL [33], Zatsepin *et al* [96], and fluxes obtained from indirect measurements by KASCADE electrons and muons for two hadronic interaction models [50] and single hadrons [97], EAS-TOP (electrons and muons) [98] and single hadrons [99], HEGRA [100], Mt. Chacaltaya [101], Mts. Fuji and Kanbala [102], Tibet burst detector (HD) [103] and AS$\gamma$ (HD) [104]. The line indicates the spectrum according to the *poly-gonato* model.

atmosphere with air shower experiments [82]. It seems that the interpretation with model 3a is better compatible with the mean logarithmic masses derived from electrons, muons, and hadrons already shown in Fig. 2 and also with the predictions of the *poly-gonato* model as indicated by the lines.

## 4. Spectra for elemental groups

A significant step forward in the understanding of the origin of cosmic rays are measurements of energy spectra for individual elements or at least groups of elements. Up to about a PeV direct measurements have been performed with instruments above the atmosphere. As examples, results for primary protons, helium, and iron nuclei are compiled in Figs. 5 to 7. Recently, also indirect measurements of elemental groups became possible.

A special class of events, the unaccompanied hadrons were investigated by the EAS-TOP and KASCADE experiments [99, 97]. Simulations reveal that these events, where only one hadron is registered in a large calorimeter, are sensitive to the flux of primary protons. The derived proton fluxes agree with the results of direct measurements as can be inferred from Fig. 5, indicating a reasonably good understanding of the hadronic interactions in the atmosphere for energies below 1 PeV.

At higher energies a breakthrough has been achieved by the KASCADE experiment.

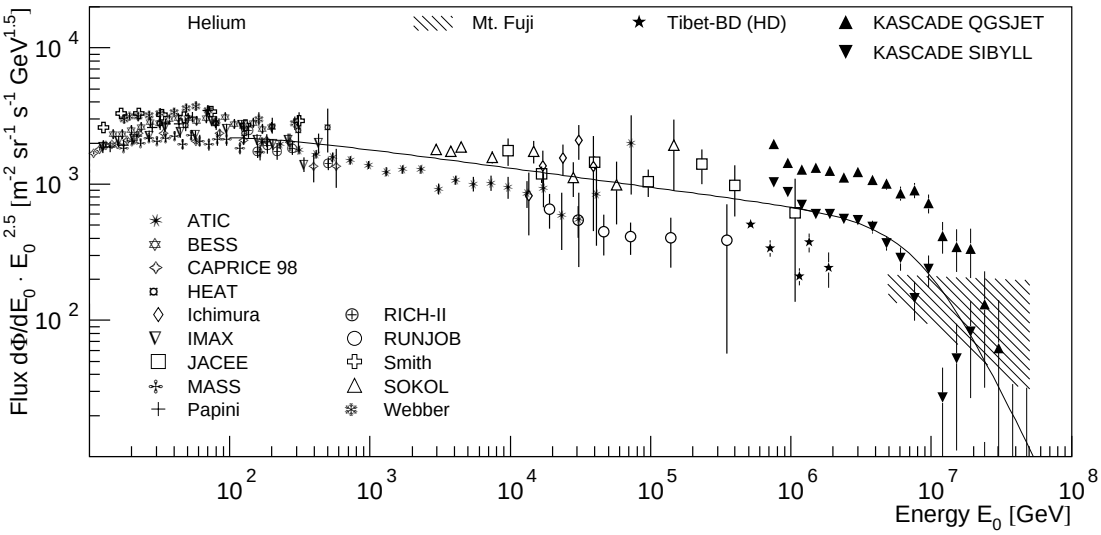


**Figure 6.** Energy spectrum for helium nuclei. Results from direct measurements above the atmosphere by ATIC [84], BESS [85], CAPRICE [86], HEAT [87], Ichimura *et al* [88], IMAX [89], JACEE [90], MASS [91], Papini *et al* [92], RICH-II [93], RUNJOB [32], Smith *et al* [95], SOKOL [33], Webber [105], and fluxes obtained from indirect measurements by KASCADE electrons and muons for two hadronic interaction models [50], Mts. Fuji and Kanbala [102], and Tibet burst detector (HD) [103]. The line indicates the spectrum according to the *poly-gonato* model.

Measuring simultaneously the electromagnetic and muonic component of air showers and unfolding the two dimensional shower size distributions, the energy spectra of five elemental groups have been derived [50]. In order to estimate the influence of the hadronic interaction models used in the simulations, two models, namely QGSJET 01 and SIBYLL [106], have been applied to interpret the measured data. It turns out that the all-particle spectra obtained agree satisfactory well within the statistical errors. For both interpretations the flux of light elements exhibits individual *knees*. The absolute flux values differ by about a factor of two or three between the different interpretations. However, it is evident that the *knee* in the all-particle spectrum is caused by a depression of the flux of light elements. The KASCADE results are illustrated in Figs. 5 to 7.

In the figures also results from other air shower experiments are shown. EAS-TOP derived spectra from the simultaneous observation of the electromagnetic and muonic components. HEGRA used an imaging Čerenkov telescope system to derive the primary proton flux [100]. Spectra for protons and helium nuclei are obtained from emulsion chambers exposed at Mts. Fuji and Kanbala [102]. The Tibet group performs measurements with a burst detector as well as with emulsion chambers and an air shower array [103, 57].

Over the wide energy range depicted, the measurements seem to follow power laws with a cut-off at high energies. The spectra according to the *poly-gonato* model are indicated in the figures as lines. It can be recognized that the measured values are compatible with cut-offs at energies proportional to the nuclear charge $\hat{E}_Z = Z \cdot 4.5$ PeV.

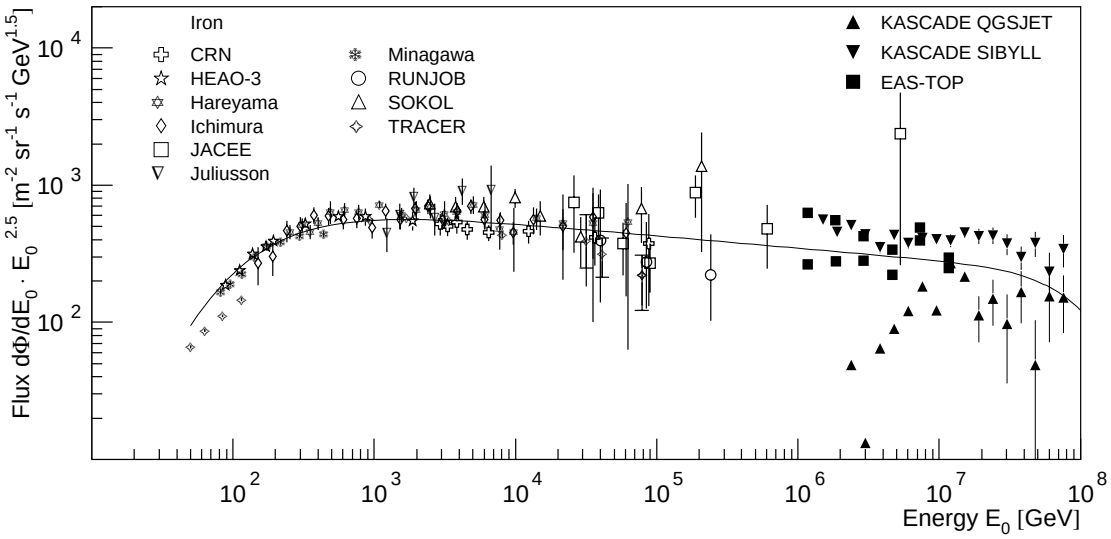


**Figure 7.** Energy spectrum for iron nuclei. Results from direct measurements above the atmosphere by CRN [107], HEAO-3 [108], Juliusson *et al* [109], Minagawa *et al* [110], TRACER [111] (single element resolution) and Hareyama *et al* [112], Ichimura *et al* [88], JACEE [31], RUNJOB [32], SOKOL [33] (iron group), as well as fluxes from indirect measurements (iron group) by KASCADE electrons and muons for two hadronic interaction models [50] and EAS-TOP [98]. The line indicates the spectrum according to the *poly-gonato* model.

## 5. Conclusion and outlook

In the last decade substantial progress has been achieved and the knowledge about galactic cosmic rays has been significantly increased. The all-particle energy spectrum is reasonably well known. For the first time, spectra for groups of elements could be derived from air shower measurements. The observed spectra seem to exhibit cut-offs proportional to the nuclear charge. The increase of the mean logarithmic mass derived from air shower observations seems to be compatible with subsequential cut-offs for individual elements. However, the interpretation of the measurements is still limited by the uncertainties of the description of hadronic interactions in the atmosphere. The implications of recent measurements on the contemporary understanding of the origin of the *knee* have been discussed elsewhere [113].

With the recent measurements of TeV $\gamma$-rays from supernova remnants [25] a new window has been opened, and the hypothesis of cosmic-ray acceleration in supernova remnants is tested directly.

With the KASCADE-Grande experiment [114], investigations of the energy spectra for groups of elements will be extended into the region of the expected iron *knee* ($\sim$ 100 PeV) and up to the second *knee* ($\sim$ 400 PeV). In particular, the inclusion of the hadronic component will help to improve the interaction models at these energies.

A new technique to measure air showers is about to be established: The LOPES experiment has registered first air showers observing geosynchrotron emission in the radio frequency range from 40 to 80 MHz [115].

The presently largest balloon borne detector, the TRACER experiment [111], almost reaches the energy region of indirect measurements. Successor experiments will provide twofold progress for the understanding of the origin of galactic cosmic rays: an extension of the measurements of the ratio of secondary to primary nuclei to energies approaching the *knee* will improve the knowledge about the propagation of cosmic rays and the extension of energy spectra with individual element resolution towards the air shower regime will provide useful information to improve hadronic interaction models.

## References


[1] J.R. Hörandel, *Astropart. Phys.* **21**, 241 (2004).
[2] E.G. Berezhko & L.T. Ksenofontov, *JETP* **89**, 391 (1999).
[3] T. Stanev *et al.*, *Astron. & Astroph.* **274**, 902 (1993).
[4] K. Kobayakawa *et al.*, *Phys. Rev. D* **66**, 083004 (2002).
[5] L.G. Sveshnikova *et al.*, *Astron. & Astroph.* **409**, 799 (2003).
[6] A.D. Erlykin & A.W. Wolfendale, *J. Phys. G: Nucl. Part. Phys.* **27**, 1005 (2001).
[7] H.J. Völk & V.N. Zirakashvili, *Proc. 28th Int. Cosmic Ray Conf., Tsukuba* **4**, 2031 (2003).
[8] W. Bednarek & R.J. Protheroe, *Astropart. Phys.* **16**, 397 (2002).
[9] S.V. Ptuskin *et al.*, *Astron. & Astroph.* **268**, 726 (1993).
[10] N.N. Kalmykov & A.I. Pavlov, *Proc. 26th Int. Cosmic Ray Conf., Salt Lake City* **4**, 263 (1999).
[11] S. Ogio & F. Kakimoto, *Proc. 28th Int. Cosmic Ray Conf., Tsukuba* **1**, 315 (2003).
[12] E. Roulet, *Int. J. Mod. Phys. A* **19**, 1133 (2004).
[13] S.P. Swordy, *Proc. 24th Int. Cosmic Ray Conf., Rome* **2**, 697 (1995).
[14] A.A. Lagutin *et al.*, *Nucl. Phys. B (Proc. Suppl.)* **97**, 267 (2001).
[15] R. Plaga, *New Astronomy* **7**, 317 (2002).
[16] S.D. Wick *et al.*, *Astropart. Phys.* **21**, 125 (2004).
[17] A. Dar, preprint astro-ph/0408310 (2004).
[18] S. Karakula & W. Tkaczyk, *Astropart. Phys.* **1**, 229 (1993).
[19] M.T. Dova *et al.*, preprint astro-ph/0112191 (2001).
[20] R. Wigmans, *Astropart. Phys.* **19**, 379 (2003).
[21] J. Candia *et al.*, *Astropart. Phys.* **17**, 23 (2002).
[22] S.I. Nikolsky *et al.*, *Phys. Atomic Nuclei* **63**, 1799 (2000).
[23] A.A. Petrukhin, *Phys. Atom. Ncl.* **66**, 517 (2003).
[24] D. Kazanas & A. Nikolaidis, *Gen. Rel. Grav.* **35**, 1117 (2001).
[25] F. Aharonian *et al.*, *Nature* **432**, 75 (2004).
[26] T. Antoni *et al.*, *Astrophys. J.* **608**, 865 (2004).
[27] M. Wiedenbeck *et al.*, *Proc. 28th Int. Cosmic Ray Conf., Tsukuba* **4**, 1899 (2003).
[28] N.E. Yanasak *et al.*, *Astrophys. J.* **563**, 768 (2001).
[29] T. Antoni *et al.*, *Astrophys. J.* **604**, 687 (2004).
[30] Grigorov *et al* after T. Shibata, *Nucl. Phys. B (Proc. Suppl.)* **75A**, 22 (1999).
[31] K. Asakimori *et al.*, *Proc. 24th Int. Cosmic Ray Conf., Rome* **2**, 707 (1995).
[32] V.A. Derbina *et al.*, *Astrophys. J.* **628**, L41 (2005).
[33] I.P. Ivanenko *et al.*, *Proc. 23rd Int. Cosmic Ray Conf., Calgary* **2**, 17 (1993).
[34] M. Takeda *et al.*, *Astropart. Phys.* **19**, 447 (2003).
[35] M. Nagano *et al.*, *J. Phys. G: Nucl. Part. Phys.* **10**, 1295 (1984).
[36] M. Nagano *et al.*, *J. Phys. G: Nucl. Part. Phys.* **18**, 423 (1984).
[37] AUGER Collaboration P. Sommers *et al.*, astro-ph/0507150 (2005).
[38] S. Ogio *et al.*, *Astrophys. J.* **612**, 268 (2004).
[39] J.W. Fowler *et al.*, *Astropart. Phys.* **15**, 49 (2001).

[40] M.A.K. Glasmacher *et al.*, *Astropart. Phys.* **10**, 291 (1999).
[41] S.P. Swordy & D.B. Kieda, *Astropart. Phys.* **13**, 137 (2000).
[42] M. Aglietta *et al.*, *Astropart. Phys.* **10**, 1 (1999).
[43] D.J. Bird *et al.*, *Astrophys. J.* **424**, 491 (1994).
[44] M.A. Lawrence *et al.*, *J. Phys. G: Nucl. Part. Phys.* **17**, 733 (1991).
[45] M. Ave *et al.*, *Astropart. Phys.* **19**, 47 (2003).
[46] F. Arqueros *et al.*, *Astron. & Astroph.* **359**, 682 (2000).
[47] T. Abu-Zyyad *et al.*, *Astrophys. J.* **557**, 686 (2001).
[48] R.U. Abbasi *et al.*, *Phys. Rev. Lett.* **92**, 151101 (2004).
[49] R.U. Abbasi *et al.*, *Astropart. Phys.* **23**, 157 (2005).
[50] H. Ulrich *et al.*, astro-ph/0505413 (2005).
[51] J.R. Hörandel *et al.*, *Proc. 26th Int. Cosmic Ray Conf., Salt Lake City* **1**, 337 (1999).
[52] T. Antoni *et al.*, *Astropart. Phys.* **16**, 245 (2002).
[53] Y.A. Fomin *et al.*, *Proc. 22nd Int. Cosmic Ray Conf., Dublin* **2**, 85 (1991).
[54] N. Ito *et al.*, *Proc. 25th Int. Cosmic Ray Conf., Durban* **4**, 117 (1997).
[55] L. Anchordoqui & H. Goldberg, *Phys. Lett. B* **583**, 213 (2004).
[56] M. Amenomori *et al.*, *Phys. Rev. D* **62**, 072007 (2000).
[57] M. Amenomori *et al.*, *Proc. 28th Int. Cosmic Ray Conf., Tsukuba* **1**, 143 (2003).
[58] D. Chernov *et al.*, astro-ph/0411139 (2004).
[59] A.V. Glushkov *et al.*, *Proc. 28th Int. Cosmic Ray Conf., Tsukuba* **1**, 389 (2003).
[60] J.R. Hörandel, *Astropart. Phys.* **19**, 193 (2003).
[61] M.A.K. Glasmacher *et al.*, *Astropart. Phys.* **12**, 1 (1999).
[62] C. Aguirre *et al.*, *Phys. Rev. D* **62**, 032003 (2000).
[63] M. Aglietta *et al.*, *Astropart. Phys.* **21**, 583 (2004).
[64] M. Aglietta *et al.*, *Astropart. Phys.* **20**, 641 (2004).
[65] K. Bernlöhr *et al.*, *Astropart. Phys.* **8**, 253 (1998).
[66] J.R. Hörandel *et al.*, *Proc. 16th European Cosmic Ray Symposium, Alcala de Henares* p. 579 (1998).
[67] K. Rawlins *et al.*, *Proc. 28th Int. Cosmic Ray Conf., Tsukuba* **1**, 173 (2003).
[68] JACEE collaboration after T. Shibata, *Nucl. Phys. B (Proc. Suppl.)* **75A**, 22 (1999).
[69] B. Wiebel-Soth *et al.*, *Astron. & Astroph.* **330**, 389 (1998).
[70] C. Büttner *et al.*, *Proc. 28th Int. Cosmic Ray Conf., Tsukuba* **1**, 33 (2003).
[71] S. Paling *et al.*, *Proc. 25th Int. Cosmic Ray Conf., Durban* **5**, 253 (1997).
[72] A.A. Watson, *Phys. Rep.* **333 - 334**, 309 (2000).
[73] T. Abu-Zayyad *et al.*, *Phys. Rev. Lett.* **84**, 4276 (2000).
[74] M. Cha *et al.*, *Proc. 27th Int. Cosmic Ray Conf., Hamburg* **1**, 132 (2001).
[75] J.E. Dickinson *et al.*, *Proc. 26th Int. Cosmic Ray Conf., Salt Lake City* **3**, 136 (1999).
[76] S. Knurenko *et al.*, *Proc. 27th Int. Cosmic Ray Conf., Hamburg* **1**, 177 (2001).
[77] J.R. Hörandel, *J. Phys. G: Nucl. Part. Phys.* **29**, 2439 (2002).
[78] D. Heck *et al.*, Report FZKA 6019, Forschungszentrum Karlsruhe (1998).
[79] N.N. Kalmykov *et al.*, *Nucl. Phys. B (Proc. Suppl.)* **52B**, 17 (1997).
[80] K. Belov *et al.*, *Nucl. Phys. B (Proc. Suppl.)* (Proc. 13th ISVHECRI) in press (2005).
[81] J.R. Hörandel, *Nucl. Phys. B (Proc. Suppl.)* (Proc. 13th ISVHECRI) in press (2005).
[82] J.R. Hörandel, *Nucl. Phys. B (Proc. Suppl.)* **122**, 455 (2003).
[83] J. Alcaraz *et al.*, *Phys. Lett. B* **490**, 27 (2000).
[84] H.S. Ahn *et al.*, *Proc. 28th Int. Cosmic Ray Conf., Tsukuba* **4**, 1833 (2003).
[85] T. Sanuki *et al.*, *Astrophys. J.* **545**, 1135 (2000).
[86] M. Boezio *et al.*, *Astropart. Phys.* **19**, 583 (2003).
[87] M.A. Du Vernois *et al.*, *Proc. 27th Int. Cosmic Ray Conf., Hamburg* **5**, 1618 (2001).
[88] M. Ichimura *et al.*, *Phys. Rev. D* **48**, 1949 (1993).
[89] M. Menn *et al.*, *Astrophys. J.* **533**, 281 (2000).

[90] K. Asakimori *et al.*, *Astrophys. J.* **502**, 278 (1998).
[91] R. Bellotti *et al.*, *Phys. Rev. D* **60**, 052002 (1999).
[92] P. Papini *et al.*, *Proc. 23rd Int. Cosmic Ray Conf., Calgary* **1**, 579 (1993).
[93] E. Diehl *et al.*, *Astropart. Phys.* **18**, 487 (2003).
[94] M.J. Ryan *et al.*, *Phys. Rev. Lett.* **28**, 985 (1972).
[95] L.H. Smith *et al.*, *Astrophys. J.* **180**, 987 (1973).
[96] V.I. Zatsepin *et al.*, *Proc. 23rd Int. Cosmic Ray Conf., Calgary* **2**, 14 (1993).
[97] T. Antoni *et al.*, *Astrophys. J.* **612**, 914 (2004).
[98] G. Navarra *et al.*, *Proc. 28th Int. Cosmic Ray Conf., Tsukuba* **1**, 147 (2003).
[99] M. Aglietta *et al.*, *Astropart. Phys.* **19**, 329 (2003).
[100] F. Aharonian *et al.*, *Phys. Rev. D* **59**, 092003 (1999).
[101] N. Inoue *et al.*, *Proc. 25th Int. Cosmic Ray Conf., Durban* **4**, 113 (1997).
[102] J. Huang *et al.*, *Astropart. Phys.* **18**, 637 (2003).
[103] M. Amenomori *et al.*, *Phys. Rev. D* **62**, 112002 (2000).
[104] M. Amenomori *et al.*, *Proc. 28th Int. Cosmic Ray Conf., Tsukuba* **1**, 107 (2003).
[105] W.R. Webber *et al.*, *Proc. 20th Int. Cosmic Ray Conf., Moscow* **1**, 325 (1987).
[106] R. Engel *et al.*, *Proc. 26th Int. Cosmic Ray Conf., Salt Lake City* **1**, 415 (1999).
[107] D Müller *et al.*, *Astrophys. J.* **374**, 356 (1991).
[108] J.J. Engelmann *et al.*, *Astron. & Astroph.* **148**, 12 (1985).
[109] E. Juliusson *et al.*, *Astrophys. J.* **191**, 331 (1974).
[110] G. Minagawa *et al.*, *Astrophys. J.* **248**, 847 (1981).
[111] D. Müller *et al.*, *Proc. 29th Int. Cosmic Ray Conf., Pune* (2005).
[112] M. Hareyama *et al.*, *Proc. 26th Int. Cosmic Ray Conf., Salt Lake City* **3**, 105 (1999).
[113] J.R. Hörandel, astro-ph/0501251 (2005).
[114] G. Navarra *et al.*, *Nucl. Instr. & Meth. A* **518**, 207 (2004).
[115] H. Falcke *et al.*, *Nature* **435**, 313 (2005).